following explicit stress–strain expressions for $a_{\gamma\gamma}$ (no summation over γ):

$$a_{\gamma\gamma} = -2C_{\mu,n}\Big[\tau S_{ij} - C_{3,n} g_n \tau^2 S_{nm} S_{nm}\left(\delta_{ij}^{(2)} - \tfrac{2}{3}\delta_{ij}^{(3)}\right) + C_{4,n} g_n \tau^2 (S_{ik}\Omega_{kj} + S_{jk}\Omega_{ki})\Big]$$

$$C_{\mu,n} = \frac{\frac{1}{2}\left(\frac{4}{3} - C_{0,n}\right) g_n}{1 - \frac{2}{3}C_{3,n}^2 g_n^2 \tau^2 S_{lm} S_{lm} + 2C_{4,n}^2 g_n^2 \tau^2 \Omega_{lm}\Omega_{lm}}$$

$$g_n = \frac{1}{C_{1,n} - 1 + P/\epsilon + f_s^{\epsilon}} \tag{6}$$

The corresponding k–ϵ model is based on the formulation by Hanjalić and Launder,[9] but includes a second source term for ϵ and the use a modified timescale. Details are given in Ref. 3.

Results

In Figs. 2a and 2b, the Reynolds stress results for the newly proposed composite model (CO) are compared to results of the original model with an isotropic dissipation (ID) and DNS data for a channel flow.[2] Because the CO and the ID models both use the same expression to calculate $\overline{uv}$, the profiles are identical. The predictions are in good agreement with the DNS data. For the normal components of $\overline{u_i u_j}$ the CO model leads to improved predictions compared to the ID model as can be seen in the examples for $\overline{uu}$ and $\overline{vv}$. Predictions of the CO model for a channel flow case at $Re_\tau = 180$ show similar features as for the high-Reynolds-number case and are, therefore, not elaborated on in this Note.

Conclusions

It is shown that a more accurate prediction of the normal stresses in the near-wall region requires an anisotropic dissipation model. Because of the lack of a model for the transport terms, which allows the explicit solution of the ARSM, these effects are often discarded. In this Note, however, it is shown that the latter assumption is not permissible in the shear direction. Hence, a new composite model formulation is presented remedying some of the previous inconsistencies. As a result, the new composite model shows improvements in modeling the normal stresses for a channel flow compared to the basic model and, therefore, promotes further studies in this direction.

References

[1]Durbin, P. A., and Speziale, C. G., "Local Anisotropy in Strained Turbulence at High Reynolds Numbers," *Journal of Fluids Engineering,* Vol. 113, No. 4, 1991, pp. 707–709.

[2]Kim, J., Moin, P., and Moser, R., "Turbulence Statistics in Fully Developed Channel Flow at Low Reynolds Number," *Journal of Fluid Mechanics,* Vol. 177, 1987, pp. 133–166.

[3]Knoell, J., and Taulbee, D. B., "A Nonlinear Stress-Strain Model for Wall-Bounded Turbulent Flows," *Engineering Turbulence Modeling and Measurements 4,* edited by W. Rodi and D. Laurence, Elsevier Science, Oxford, 1999, pp. 103–112.

[4]Taulbee, D. B., "An Improved Algebraic Reynolds Stress Model and Corresponding Nonlinear Stress Model," *Physics of Fluids A,* Vol. 4, No. 11, 1992, pp. 2555–2561.

[5]Rodi, W., "A New Algebraic Relation for Calculating the Reynolds Stresses," *ZAMM,* Vol. 56, No. 3, 1976, pp. T219–T221.

[6]Pope, S. B., "A More General Effective-Viscosity Hypothesis," *Journal of Fluid Mechanics,* Vol. 72, No. 2, 1975, pp. 331–340.

[7]Hanjalić, K., and Jakirlić, S., "A Model of Stress Dissipation in Second-Moment Closures," *Applied Scientific Research,* Vol. 51, 1993, pp. 513–518.

[8]Ni, W., "Nonlinear Eddy-Viscosity Turbulence Model and Its Application," *AIAA Journal,* Vol. 37, No. 8, 1999, pp. 1000–1002.

[9]Hanjalić, K., and Launder, B. E., "A Reynolds Stress Model of Turbulence and Its Application to Thin Shear Flows," *Journal of Fluid Mechanics,* Vol. 52, No. 4, 1972, pp. 609–638.

J. P. Gore
Associate Editor

Direct Circulation Measurement of a Tip Vortex

K. J. Desabrais* and H. Johari†
Worcester Polytechnic Institute, Worcester, Massachusetts 01609

Introduction

THE circulation of tip vortices has traditionally been calculated by taking the line integral of the velocity around a closed path surrounding the vortex, which requires detailed knowledge of the velocity field. Measurements of the velocity field can be made by either single-point anemometry or whole-field particle image velocimetry (PIV) techniques. Alternatively, if vortex circulation is the primary parameter of interest, the direct measurement of circulation can be achieved via acoustic means, thus eliminating the need for detailed velocity measurements. An acoustic method that allows for a simple, nonintrusive method of circulation measurement has been developed in our laboratory utilizing narrow ultrasound beams.[1] This method significantly decreases the time it takes to find the circulation in a specified region of the flow. The method has been used to measure the circulation of delta wing vortices[2] and the bound circulation of an airfoil.[1] This method was utilized in the current study to examine the circulation of a tip vortex.

Tip vortices have been studied extensively in the past. Most of the studies have examined the behavior of vortices using classical anemometry techniques.[3–6] More recently, PIV has been employed to obtain detailed velocity field measurements of the tip vortex in the near field[7] and the far field.[8] Various vortex characteristics such as circulation have been extracted from these velocity fields. The vortex circulation measured by our ultrasound method is compared against previous data to assess the applicability of the ultrasound technique.

Ultrasound Method

The ultrasound technique is based on the time of flight of sound pulses traversing a given path. Sound travels through fluids with a velocity that is the sum of the local sound speed and the local flow velocity. If the local flow velocity augments (retards) the sound speed, the time of flight would be decreased (increased). In our setup, a sound pulse was transmitted around a closed rectangular path in one direction, and its transit time was accurately measured. The process was then repeated by emitting a pulse in the opposite direction around the closed path. In the presence of a vortex, a time difference Δt would be generated from transversing the path in opposite directions. As derived by Johari and Durgin,[1] the net circulation Γ is linearly proportional to the time difference, that is, $\Gamma = \frac{1}{2}a^2\Delta t$, as long as the sound speed a is constant along the path during the transit time and the velocity component along the acoustic path is small, for example, less than $0.1a$. Further details of the method, its advantages, and limitations are discussed by Johari and Durgin.[1]

Experimental Setup

The experiments were conducted in the Worcester Polytechnic Institute low-speed wind tunnel that has test section dimensions of 45.7 cm high × 61.0 cm wide × 91.4 cm long. To create a tip vortex, a half-wing was mounted vertically from the tunnel ceiling. The wing was a blunt-ended, rectangular planform NACA 0012 with a chord c of 10.5 cm and a semispan s of 22.3 cm resulting in a (half-wing) aspect ratio of 2.1. The angle of attack was measured

Received 16 August 1999; revision received 6 July 2000; accepted for publication 21 July 2000.

*Graduate Student, Mechanical Engineering Department. Student Member AIAA.

†Associate Professor, Mechanical Engineering Department. Senior Member AIAA.

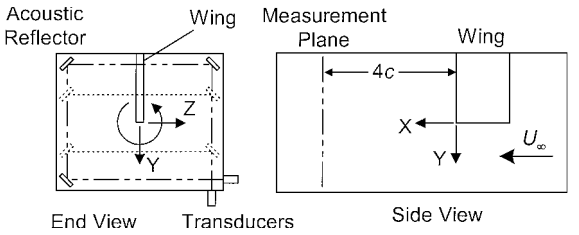

Fig. 1 Schematic of experimental apparatus and acoustic measurement plane.

using a rotary position sensor with an accuracy of ±0.1 deg. Two angles of attack of 5 and 10 deg were examined at freestream velocities of 10 and 15 m/s, corresponding to chord Reynolds numbers of 6.8×10^4 and 1.0×10^5.

An acoustic path was created in a plane perpendicular to the freestream by employing two transducers and three reflectors. The acoustic reflectors were positioned at four chords downstream of the trailing edge of the wing. The length of the wind-tunnel test section permitted measurements only in the near-field region of the tip vortex. The measurement plane and the coordinate system are shown in Fig. 1. The reflectors were mounted such that the upper two reflectors were movable in the y direction, which allowed for changes in the acoustic path length and the enclosed area. This permitted the measurement of the distribution of the vortex circulation. The two transducers were mounted flush with the (inside) tunnel walls, and the distance between the reflectors in the z direction was fixed at 47.6 cm. This arrangement produced a closed path that did not include the boundary layers on the tunnel walls. With the measurement plane located four chords downstream of the trailing edge of the wing, the vortex is expected to be well formed and axisymmetric.[6,7] Vortex wandering effects are also small at this station.[6]

The ultrasound measurements were made using a pair of 19-mm-diam transducers operating at a frequency of 100 kHz (Ref. 9). The transducers were operated by an ultrasonic controller that served also as a timing device. Calibration in still air showed that it had a timing uncertainty of 5×10^{-8} s, which corresponds to a minimum circulation uncertainty of ±.003 m^2/s at room temperature. This was significantly less than one standard deviation of the measured data.

Results

The circulation distribution of the wing tip vortex was measured by varying the path of the ultrasound beam. As shown in Fig. 2, the position of one leg of the ultrasound path was varied from a path that completely encompassed the vortex to a position where the vortex was completely outside the path. At each position, approximately 100 data points were recorded. A sample circulation distribution is shown in Fig. 2. The error bars represent plus and minus one standard deviation of the measurements, and the mean uncertainty for the measurements is 5%.

The circulation distribution shows that the maximum circulation was maintained at a nearly constant level when the path completely surrounded the vortex core. Circulation dropped sharply through the vortex core, and once the ultrasound path was completely outside the vortex, the circulation approached zero. These results are expected because, when the ultrasound path completely encompasses the vortex, all of the vorticity is contained inside the path and the highest circulation values are achieved. When the ultrasound path passes through the vortex core, some of the vorticity is no longer enclosed by the path and so the circulation will be lower. Once the path is outside of the vortex, the circulation approaches zero. The small dip in the data at $y/c \approx -1.0$ corresponds to the position where a pitot tube was mounted in the tunnel upstream of the measurement plane. The pitot tube wake reduced the circulation at this point.

The measured circulation values for the four cases were normalized with the chord length, freestream velocity, and sectional lift coefficient, that is, $\Gamma/cU_\infty c_l = \Gamma/2\Gamma_{\text{bound}}$. Here Γ_{bound} is the measured bound circulation of the NACA 0012 airfoil.[1] The normalized circulation distributions presented in Fig. 3 show reasonable agreement among the four cases studied. This normalization scheme appears to collapse the data over the conditions studied and reveals that about

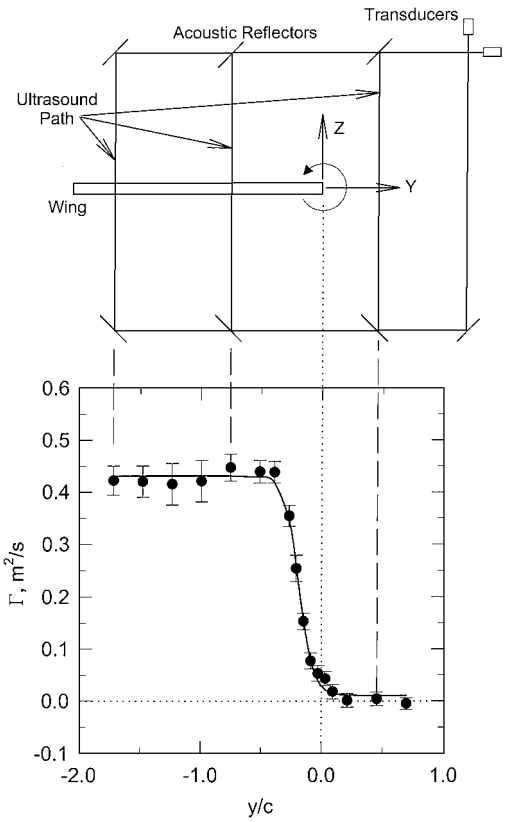

Fig. 2 Circulation distribution for a tip vortex at $Re_c = 6.8 \times 10^4$ and $\alpha = 10$ deg.

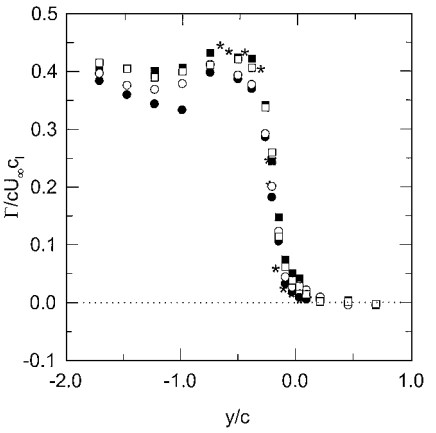

Fig. 3 Normalized circulation distribution of tip vortices: ●, $Re_c = 6.8 \times 10^4$ and $\alpha = 5$ deg; ■, $Re_c = 6.8 \times 10^4$ and $\alpha = 10$ deg; ○, $Re_c = 1.0 \times 10^5$ and $\alpha = 5$ deg; □, $Re_c = 1.0 \times 10^5$ and $\alpha = 10$ deg; and ∗, Vogt et al.[7] $Re_c = 1.5 \times 10^5$ and $\alpha = 10$ deg.

80% of the wing circulation was rolled up into the tip vortex at $x/c = 4$. The dip in the data at $y/c \approx -1.0$ in Fig. 3 corresponds to the pitot tube location for all four cases presented.

PIV measurements of a tip vortex generated by a NACA 0012 wing at four chords downstream of the trailing edge were performed by Vogt et al.[7] at a Reynolds number of 1.5×10^5 and 10-deg angle of attack. The effects of vortex wandering were removed by aligning the vortex centers of 1000 individual PIV velocity fields before averaging them. The properly averaged data field was acquired, and contour integrations corresponding to our acoustic paths were performed. This way, circulation distributions obtained from the ultrasound method can be compared directly against those from velocity measurements. The circulation distribution of the PIV data is also included in Fig. 3. The measurements obtained from the PIV data correlate well with the ultrasound measurements providing support that the ultrasound method accurately measures the circulation distribution of the tip vortex.

Table 1 Tip vortex characteristics

Case	U_∞, m/s	Re_c	α, deg	$\Gamma_v/(cU_\infty c_l)$	$-y_c/s$	d/s
1	10	6.8×10^4	5	0.38	0.10	0.15
2	10	6.8×10^4	10	0.41	0.09	0.17
3	15	1.0×10^5	5	0.40	0.10	0.17
4	15	1.0×10^5	10	0.42	0.09	0.14
PIV[7]	25	1.5×10^5	10	0.43	——	0.05

The maximum vortex strength $\Gamma_v/(cU_\infty c_l)$, core location y_c/s, and vortex diameter d/s, listed in Table 1, were extracted from the circulation distributions by fitting hyperbolic tangent curves to the data. The spanwise location where Γ was one-half of its maximum value yielded y_c, and the vortex diameter was the extent between the 5 and 95% circulation values. The experimental uncertainty is 5% for the former two parameters; the vortex diameter uncertainty is much more difficult to quantify because of the asymptotic nature of the curve fit at the two ends.

The normalized maximum vortex strength remains nearly constant (within ±5%) for the four cases considered. The vortex strength of the PIV data shows good agreement with the data at 10 deg, which suggests that the ultrasound method accurately measured the total circulation of the tip vortex. Because of the wandering correction, comparison of the acoustically measured core location with the PIV data would not be appropriate, as indicated in Table 1.

The normalized vortex diameter varied over a range of values and was about three times larger than that from the PIV data. The asymptotic nature of the curve fit at the two extremes makes this parameter very sensitive to small variations in the data. Additionally, the sound pulses had a scale (the diameter of the transducer face) on the order of 2 cm that tends to limit the spatial resolution of the measurements and to result in larger vortex diameters. The vortex diameter based on the maximum tangential velocity reported in Ref. 6 is generally on the order of 10% of the wing span, which corresponds to about 2 cm for our setup. This suggests that the vortex diameter measured in the present experiments was approximately the same size as the sound pulse used to measure the circulation. This is the reason for the larger vortex diameters inferred. The relative spatial resolution of the system would be improved in a larger experimental setup.

Forcing of the vortex was pursued in an attempt to alter the vortex characteristics. The forcing was accomplished by steady and pulsatile injection, as well as suction of air (in the freestream direction) from the vortex core. For the conditions utilized, no changes were found in the forced vortex characteristics over the baseline case at the four-chord measurement location.[9]

Summary

The circulation distribution of a wing tip vortex as a function of the spanwise coordinate was measured directly by an ultrasound technique utilizing a rectangular acoustic path. The vortex was generated by a blunt-ended NACA 0012 half-wing, and the measurements were made at four chords downstream of the trailing edge. The circulation distribution behaved as expected: achieving its highest level when the rectangular integration path completely surrounded the vortex. The circulation decreased rapidly through the vortex center before reaching nearly zero when one side of the integration path traversed through the vortex. The direct acoustic measurements of circulation agreed well with those derived from detailed velocity field data generated by a similar wing. The ultrasound method offers accurate circulation measurements as long as the flow scales are larger than the size of the sound pulse employed in the measurements.

Acknowledgments

The first author was supported by the Massachusetts Space Grant Consortium. We would like to thank M. Gharib of the California Institute of Technology for providing us the PIV data.

References

[1] Johari, H., and Durgin, W. W., "Direct Measurement of Circulation Using Ultrasound," *Experiments in Fluids*, Vol. 25, No. 5/6, 1998, pp. 445–454.

[2] Johari, H., and Moreira, J., "Direct Measurement of Delta-Wing Vortex Circulation," *AIAA Journal*, Vol. 36, No. 12, 1998, pp. 2195–2203.

[3] Corsiglia, V. R., Schwind, R. G., and Chigier, N. A., "Rapid Scanning, Three-Dimensional Hot-Wire Anemometer Surveys of Wing-Tip Vortices," *Journal of Aircraft*, Vol. 10, No. 12, 1973, pp. 752–757.

[4] Baker, G. R., Barker, S. J., Bofah, K. K., and Saffman, P. G., "Laser Anemometer Measurements of Trailing Vortices in Water," *Journal of Fluid Mechanics*, Vol. 65, Pt. 2, 1974, pp. 325–336.

[5] Ciffone, D. L., and Orloff, K. L., "Far-Field Wake Vortex Characteristics of Wings," *Journal of Aircraft*, Vol. 12, No. 5, 1975, pp. 464–470.

[6] Devenport, W. J., Rife, M. C., Liapis, S. I., and Follin, G. J., "The Structure and Development of a Wing-Tip Vortex," *Journal of Fluid Mechanics*, Vol. 312, 1996, pp. 67–106.

[7] Vogt, A., Baumann, P., Gharib, M., and Kompenhans, J., "Investigations of a Wing Tip Vortex in Air by Means of DPIV," AIAA Paper 96-2254, June 1996.

[8] Jacob, J., Savaş, Ö., and Liepmann, D., "Trailing Vortex Wake Growth Characteristics of a High Aspect Ratio Rectangular Airfoil," *AIAA Journal*, Vol. 35, No. 2, 1997, pp. 275–280.

[9] Desabrais, K. J., and Johari, H., "Direct Circulation Measurement of a Wing Tip Vortex Using Ultrasound," AIAA Paper 98-0609, Jan. 1998.

A. Plotkin
Associate Editor

Optimal Structural Control by Substructure Synthesis

M. Sunar*
King Fahd University of Petroleum and Minerals, Dhahran 31261, Saudi Arabia
and
S. S. Rao†
University of Miami, Coral Gables, Florida 33124

Introduction

SUBSTRUCTURAL decomposition techniques have been developed for large flexible structures to reduce the order of their full model to a manageable level. These techniques were applied to the control of large flexible structures by Pan[1] and Sunar and Rao[2] using the linear quadratic regulator control method and by Su et al.[3] using the linear quadratic Gaussian (LQG) control method.

In this Note, a generalized substructural decomposition technique is presented to efficiently design controllers and observers for large flexible structures using the LQG method. The structure is decomposed into substructures and the equations of motion (EOM) are written for all of the substructures. The boundary forces due to subcontrollers of surrounding substructures are included in the EOM as they become available. These EOM are used in the subcontroller and subobserver designs for all of the substructures. The subcontroller and subobserver matrices are assembled to obtain the global controller for the whole structure. The accuracy and efficiency of the substructural technique as compared to the full structural model are numerically illustrated on a large flexible structure.

Substructure Decomposition and Nodal Condensation

Assume that a flexible structure is decomposed into r substructures. The partitioned EOM of any kth substructure in the configuration space with only controller input $\boldsymbol{u}$ can be written as

$$\begin{bmatrix} M_{A_kA_k} & M_{A_kB_k} \\ M_{B_kA_k} & M_{B_kB_k} \end{bmatrix} \begin{Bmatrix} \ddot{\boldsymbol{d}}_{A_k} \\ \ddot{\boldsymbol{d}}_{B_k} \end{Bmatrix} + \begin{bmatrix} C_{d_{A_kA_k}} & C_{d_{A_kB_k}} \\ C_{d_{B_kA_k}} & C_{d_{B_kB_k}} \end{bmatrix} \begin{Bmatrix} \dot{\boldsymbol{d}}_{A_k} \\ \dot{\boldsymbol{d}}_{B_k} \end{Bmatrix} + \begin{bmatrix} K_{A_kA_k} & K_{A_kB_k} \\ K_{B_kA_k} & K_{B_kB_k} \end{bmatrix} \begin{Bmatrix} \boldsymbol{d}_{A_k} \\ \boldsymbol{d}_{B_k} \end{Bmatrix} = \begin{bmatrix} D_{A_kA_k} & D_{A_kB_k} \\ D_{B_kA_k} & D_{B_kB_k} \end{bmatrix} \begin{Bmatrix} \boldsymbol{u}_{A_k} \\ \boldsymbol{u}_{B_k} \end{Bmatrix} \quad (1)$$

Received 14 April 2000; accepted for publication 27 July 2000.

*Assistant Professor, Mechanical Engineering Department.
†Professor and Chairman, Department of Mechanical Engineering.